Materials Science in Semiconductor Processing 26 (2014) 238–243

Contents lists available at ScienceDirect

Materials Science in Semiconductor Processing

journal homepage: www.elsevier.com/locate/mssp

The photovoltaic performance of alloyed $CdTe_xS_{1-x}$ quantum dots sensitized solar cells

N. Al-Hosiny [a,c], S. Abdallah [a,b,*], Ali Badawi [a], K. Easawi [b], H. Talaat [d]

[a] Department of Physics, Faculty of Science, Taif University, Taif, Saudi Arabia
[b] Department of Mathematical and Physical Engineering, Faculty of Engineering (Shoubra), Benha University, Cairo, Egypt
[c] Department of Physics, Faculty of Science, Aljouf University, Aljouf, Saudi Arabia
[d] Department of Physics, Faculty of Science, Ain Shams University, Abbassia, Cairo, Egypt

ARTICLE INFO

Available online 21 May 2014

Keywords:
Alloyed $CdTe_xS_{1-x}$ quantum dots sensitized solar cells
Direct adsorption
Photovoltaic performance

ABSTRACT

The photovoltaic performance of alloyed $CdTe_xS_{1-x}$ quantum dots (QDs) sensitized solar cells (QDSSCs) as a function of tuning the band gap of alloyed $CdTe_xS_{1-x}$ QDs is studied. The tuning of band gap was carried out through controlling the molar ratio (x) of QDs. Presynthesized alloyed $CdTe_xS_{1-x}$ QDs of different x values (0, 0.2, 0.4, 0.6, 0.8, and 1) were deposited by direct adsorption (DA) technique onto a layer of TiO_2 nanoparticles (NPs) to serve as sensitizers for the solar cells. The characteristic parameters of the assembled QDSSCs were measured under AM 1.5 sun illumination, and show that $CdTe_xS_{1-x}$ QDs has better photovoltaic performance than pure CdTe QDs or CdS QDs. The maximum values of J_{sc} (1.54 mA/cm^2) and η (0.31%) were obtained for $x=0.6$. However, The open circuit voltages (V_{oc}) approximately constant (0.46 ± 0.02 V) for all alloyed $CdTe_xS_{1-x}$ QDSSCs. It is only dictated by the conduction band (CB) level of TiO_2 nanoparticles (NPs) and the valance band (VB) of the electrolyte.

1. Introduction

In recent years, there has been a concerted effort to enhance the performance of quantum dot sensitized solar cells (QDSSCs) [1–3]. Semiconductor quantum dots (QDs) exhibit attractive characteristics as sensitizers in solar cells applications due to their tunable band gaps through size control to match the solar spectrum [1,4]. However, this characteristic may cause problems in solar cells' applications. In the case of small particles (less than 2 nm in size) with a short emission wavelength, the optical properties are unstable. To overcome such problems, a new class of alloyed semiconductor QDs has been studied, that provide a way for continuous tuning of the effective band gap without changing the particle size. The band gap of $CdTe_xS_{1-x}$ alloyed QDs can be adjusted by varying the tellurium concentration [5,6], spanning the compositional range from pure CdS ($x=0$) to pure CdTe ($x=1$), giving band gap energies that ranges from the UV to the visible spectrum. This makes $CdTe_xS_{1-x}$ a potentially favorable material as a sensitizer for QDs sensitized solar cells (QDSSCs). Many studies were carried out on photovoltaic cells using QDs such as CdSe [7,8], CdS [9–11], CdTe [2,12], PbS [13], PbSe [14], InAs [15], $Cu_{2-x}S$ [16], Ag_2Se [17], and Ag_2S [1] for harvesting solar radiation in the visible and infrared regions. In the case of QDSSCs, excited electrons of semiconductor nanocrystals are injected into a large band gap semiconductor such as TiO_2 or ZnO, while holes are scavenged by a redox couple. Since QDSSCs have large surface areas, they would provide a technically and economically credible alternative to conventional cells;

* Corresponding author at: Department of Physics, Faculty of Science, Taif University, Taif, Saudi Arabia. Tel.: +966 55 36 802 01; fax: +966 272 41880.
E-mail address: dr.saiedabdallah@yahoo.com (S. Abdallah).

http://dx.doi.org/10.1016/j.mssp.2014.05.017
1369-8001/

silicon photovoltaic or dye-sensitized solar cells (DSSCs). The latter cells have many limitations, such as difficulties in utilizing the infra-red region of the solar spectrum, and instability for long-term uses. The band gap of $CdTe_xS_{1-x}$ alloyed NCs can be adjusted by varying the tellurium molar ratio, spanning the compositional range from pure CdS ($x=0$) to pure CdTe ($x=1$), where the band gap energies ranges from the UV to Near Infra Red region. These properties make its' QDs a good absorber for the visible region in solar spectrum, capable of effectively injecting electrons into TiO_2 NPs. Many methods are used to anchor QDs onto the large band gap metal oxides. Normally, these adsorption methods are: (1) in situ growth of QDs by either chemical bath deposition (CBD) technique [1,18], containing both the cationic and anionic precursors, or successive ionic layer adsorption and reaction deposition (SILAR) method [19,20], (2) *ex situ* growth as electrophoretic deposition (EPD) method [21,22], linker-assisted adsorption (LA) [23], and direct adsorption (DA) technique [10,24].

In this work, we prepared alloyed $CdTe_xS_{1-x}$ QDs of approximately the same sizes by organometallic pyrolysis method to be used as a sensitizers in QDSSCs. These colloidal QDs were adsorbed onto TiO_2 NPs by DA technique at 24 h dipping time under ambient conditions. The effect of the molar ratio (x) on the QDSSCs characteristic parameters; short circuit current density (J_{sc}), open circuit voltage (V_{oc}), fill factor (FF), and efficiency (η) for energy conversion were studied.

2. Experiment

2.1. Preparation of $CdTe_xS_{1-x}$ quantum dots

A series of alloyed $CdTe_xS_{1-x}$ NCs samples ($x=0$, 0.2, 0.4, 0.5, 0.6, 0.8, and 1.0) were synthesized as the method of Talapin et al. [25] by varying the amount of the second precursor. Cadmium solution was prepared by 0.3 g of CdO added to 3.0 g of stearic acid, and heated up to 170 °C till the red color of CdO disappears to ensure that the reaction between CdO and stearic acid is complete and CdO completely transform to Cd sterate. 2.0 g of tri-*n*-octylphosphine oxide (TOPO) and 1.0 g of hexadecyleamine (HDA) were added to the reaction mixture and heated at 200 °C. For example in the preparation of $CdTe_{0.4}S_{0.6}$ NCs sample, Tellurium solution was prepared by mixing 0.53 g of tellurium in 1.5 mL of trioctylphosphine (TOP). Sulfur solution was also prepared by dissolving 0.2 g of sulphur in 1.5 mL of TOP. The mixture was then injected into the cadmium solution at 200 °C. Appropriate amounts of sulfur and tellurium solutions were mixed together to give the above ratios. Six samples with different molar ratios ($x=0$, 0.2, 0.4, 0.6, 0.8, and 1) were obtained from the reaction mixture at time interval of 7 min and labeled from a to f. The samples were separated using centrifuge followed by surface treatment according to the method of Choi et al. [26]. Each sample of alloyed QDs was washed several times with methanol to remove excess ligands, then TOP/TOPO or TOPO/DDA ligands on the surface of alloyed QDs were replaced by refluxing the QDs in pyridine (20 mL) under 1 atm of N_2 for 24 h. The QDs were precipitated with toluene at room temperature.

2.2. Preparation of solar cell electrodes

The TiO_2 colloidal paste was prepared by the method of Syrrokostas et al. [27]. Three grams of commercial TiO_2 nanopowder (20 nm) (Degussa P-25) was ground in a porcelain mortar and mixed with a small amount of distilled water (1 mL) containing acetyl acetone (10% v/v) to create the paste. Acetyl acetone was used as a dispersing agent, since it prevents coagulation of TiO_2 nanoparticles and affects the porosity of the film. The paste was diluted further by slow addition of distilled water (4 mL) under continued grinding. The addition of water controls the viscosity and the final concentration of the paste. Finally, few drops of a detergent (Triton X-100) were added to facilitate the spreading of the paste on the substrate, since this substance has the ability to reduce surface tension, resulting in even spreading and reducing the formation of cracks. The TiO_2 paste was deposited on a conducting glass substrate of SnO_2:F with sheet resistance of 7 Ω/sq and $>80\%$ transmittance in the visible region, using a simple doctor blade technique. This was followed by annealing at 450 °C for 30 min. and the final thickness was 8 μm after the solvent evaporation. Then the TiO_2 films were dipped into a colloidal solution of pre-synthesized alloyed $CdTe_xS_{1-x}$ QDs to form the working electrodes. The counter electrodes were prepared by coating another FTO substrate sheet with Pt.

2.3. Assembly of QDSSC

The Pt counter electrode and alloyed $CdTe_xS_{1-x}$ sensitized TiO_2 electrode were assembled as a sandwich type cell using clamps. Both electrodes were sealed using a hot-melt polymer sheet (solaronix, SX1170-25PF) of 25 μm thickness in order to avoid evaporation of the electrolyte. Finally, Iodide electrolyte solution was prepared by dissolving 0.127 g of 0.05 M Iodine (I_2) in 10 mL of water-free ethylene glycol, then adding 0.83 g of 0.5 M potassium iodide (KI). The electrolyte was inserted in the cell with a syringe, filling the space between the two electrodes.

2.4. Measurements

The sizes of the alloyed QDs were measured by high resolution transmission electron microscope (HRTEM) (JEOL JEM-2100 operated at 200 kV and equipped with Gatan CCD high resolution camera). X-ray diffraction (XRD) patterns were carried out with an automated powder diffractometer (Bruker D8-advace diffractometer) with Cu X-ray tube (Wavelength: $k\alpha 1=1.540598$), the tube potential is 40 kV and the tube current is 40 mA. The absorption spectra of the alloyed $CdTe_xS_{1-x}$ QDs (before and after adsorption on TiO_2 electrodes) were recorded using a UV–Vis. spectrophotometer (JASCO V-670). Light emission observed under 472 nm LED lamp. In addition, the current density–voltage (J–V) characteristics were recorded with a Keithley 2400 voltage source/ammeter using GreenMountain IV-Sat 3.1 software. The alloyed

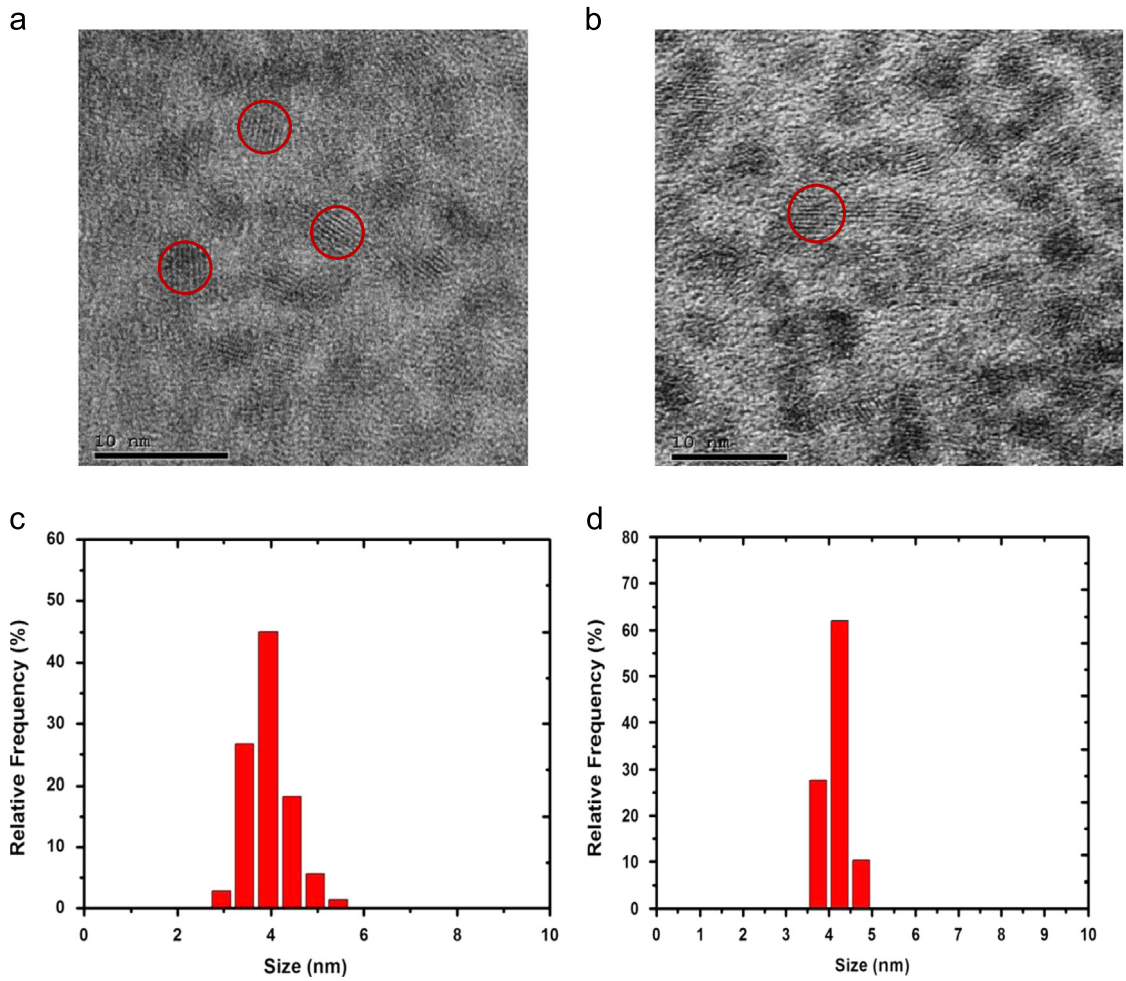

Fig. 1. HRTEM images and the corresponding histogram for $CdTe_xS_{1-x}$ for: (a) $x=0.2$ and (b) $x=0.8$, c and d are their corresponding histograms, respectively.

$CdTe_xS_{1-x}$ QDSSCs were subjected to the irradiation of a solar simulator (ABET technologies, Sun 2000 Solar Simulators, USA) operating at 100 mW/cm^2 (AM1.5G). A Leybold certified silicon reference solar cell (Model: [57863]) were used to calibrate the incident solar illumination. A *J–V* characteristic curve of each molar ratios (*x* values) of alloyed $CdTe_xS_{1-x}$ QDSSC was studied, and experiments were carried out under ambient conditions.

3. Results and discussion

3.1. Characterization of the $CdTe_xS_{1-x}$ QDs

The average particle size distributions of the samples were measured using HRTEM (JEOL 311UHR operated at 300 kV). Specimens were prepared by depositing a drop of hexane solution onto a Formvar-coated copper grid and letting it to dry in air. Fig. 1((a) and (b)) shows the HRTEM micrographs for alloyed $CdTe_xS_{1-x}$ QDs for $x=0$. 2, and 0.8 respectively as an examples. While Fig. 1(c) and (d) show their corresponding histogram of particle size distribution for the same samples respectively. The sizes of alloyed NCs are: 3.9, 3.95, 4.02, 3.85, 4.1, and 4.0 nm for $x=0$, 0.2, 0.4, 0.6, 0.8, and 1, respectively. It is observed that the average particles sizes of all samples are approximately equal and the small variations are within the experimental error (3.97 ± 0.30 nm). Ultrahigh resolution images of the 10 nm nanoparticle are showing the crystal lattice planes.

The prepared alloyed $CdTe_xS_{1-x}$ samples were characterized using X-ray diffraction. The diffraction patterns seemed to be single phase with cubic sphalerite structure only. However, trials to apply MAUD program for Rietveld analysis yield bad pattern fitting as a single phase. So, we applied X'pert HighScore Plus program to identify the phases present in the samples. Two phases were identified, CdS wurtzite hexagonal structure and CdTe cubic structure. The phase composition and crystal structure of one of the samples $CdTe_{0.6}S_{0.4}$ is further investigated applying Rietveld method. Fig. 2 illustrates the pattern fitting resulting from the Rieveld analysis. The analysis yields a phase percentage of 58.2% for CdTe (International Centre for Diffraction Data (ICDD) No. 15-0770) [28] and

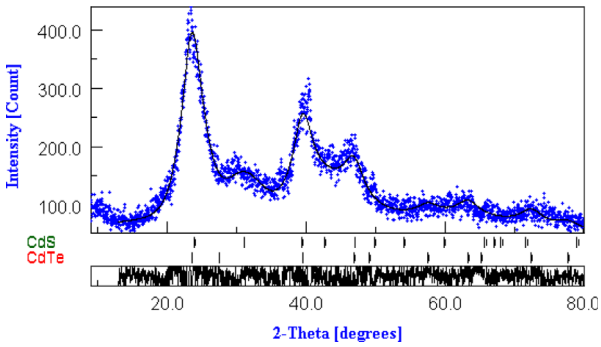

Fig. 2. XRD pattern of alloyed $CdTe_xS_{1-x}$ (x=0.6) QDs.

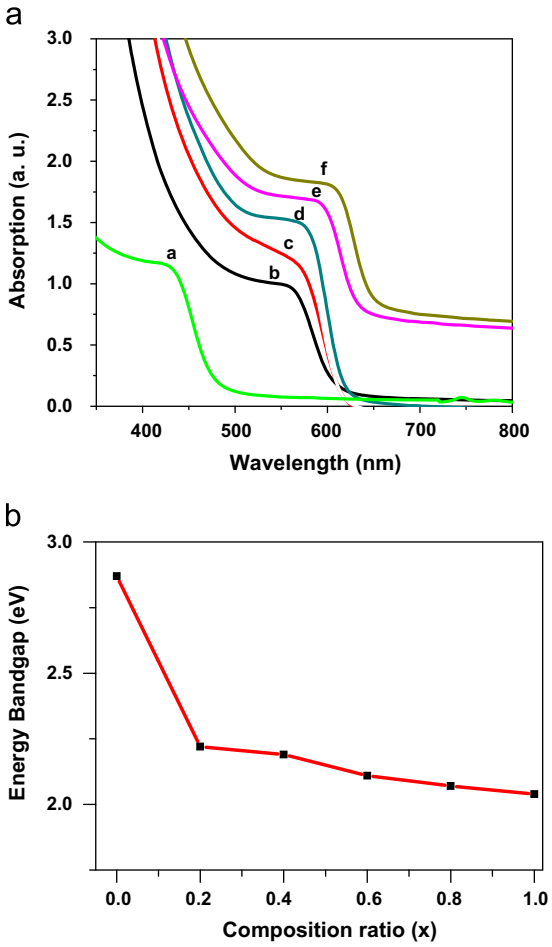

Fig. 3. (a) UV–Vis absorption spectra for alloyed $CdTe_xS_{1-x}$ QDs samples (a–f), (b) Alloyed $CdTe_xS_{1-x}$ QDs bandgap vs. composition ratio (x).

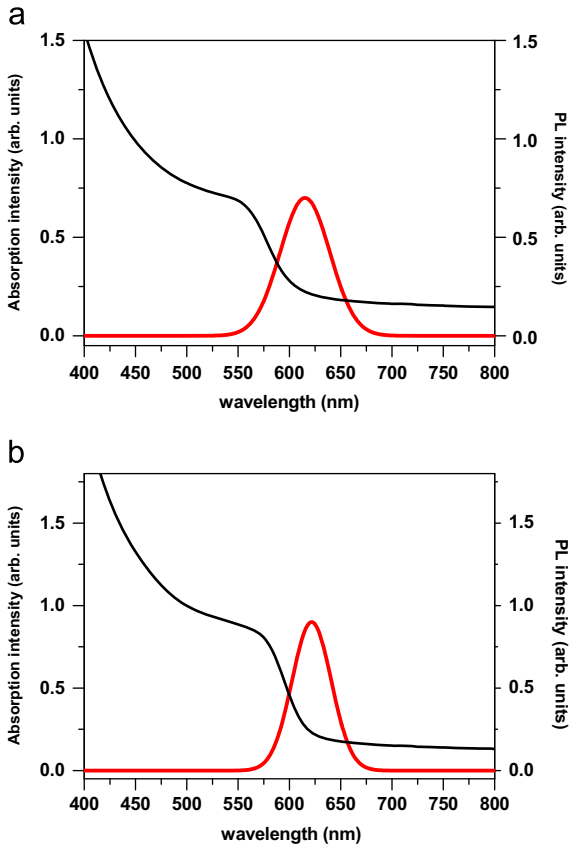

Fig. 4. The absorption (black line) and the emission (red line) for $CdTe_xS_{1-x}$ sample (a) x=0.2 and (b) x=0.6. (For interpretation of the references to color in this figure legend, the reader is referred to the web version of this article.)

41.2% for CdS (ICDD No. 75-1546) [28], which indicate that the ternary alloy are formed.

Fig. 3(a) shows UV–Vis. absorption of the alloyed $CdTe_xS_{1-x}$ QDs. It can be seen, as x value increase, the absorption peak red-shifts from 431 nm (a) to 605 nm (f). The corresponding energy gaps are 2.87 eV and 2.04 eV, respectively. The red-shift of the UV–Vis. absorption spectra of the alloyed $CdTe_xS_{1-x}$ NCs with increasing Te content is due to the decrease of the band gap caused by the incorporation of Te (as shown in Fig. 3(b)).

The absorption and the emission spectra for the samples $CdTe_xS_{1-x}$ (x=0.2, 0.6) as examples are shown in Fig. 4(a) and (b). The excitation wavelength is 472 nm from LED lamp. It can be seen that the photoluminescence (PL) peak at lower energy (longer wavelength) than absorbance. The symmetric

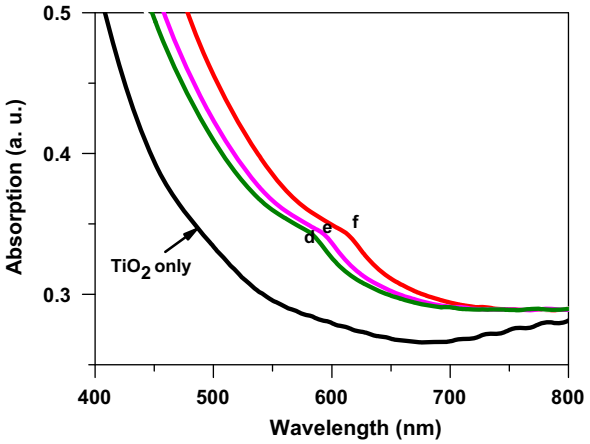

Fig. 5. UV–Vis absorption spectra of TiO_2 NCs film and alloyed $CdTe_xS_{1-x}$ QDs/TiO_2 for different values of x (0, 0.6, 0.8 and 1.0).

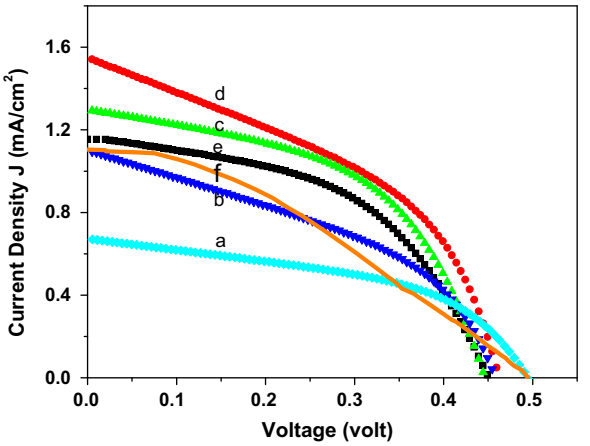

Fig. 6. *J–V* characteristic curves of alloyed $CdTe_xS_{1-x}$ QDs QDSSCs (a–f) for solar illumination of 100 mW/cm^2.

and narrow PL spectra indicate the good quality and few electronic defect site in the alloyed NCs.

3.2. Characterization of alloyed $CdTe_xS_{1-x}$ QDs sensitized TiO_2 electrodes (the working electrode)

To ensure, that the adsorption of alloyed QDs onto the TiO_2 electrode takes place, the absorption spectra of the working electrodes of $CdTe_xS_{1-x}/TiO_2$ for samples d (x=0.6), e (x=0.8) and f (x=1) were measured and shown in Fig. 5. It is seen that the absorption edges are 583 nm, 695 nm, and 615 nm for samples d, e and f, respectively. These absorption edges are in good agreement with those obtained for the same samples in colloidal solution indicating the better adsorption of alloyed QDs in the nanoporous TiO_2 electrode. The slight shift of the absorption edges may be due to the change of the alloyed $CdTe_xS_{1-x}$ QDs size.

3.3. Characterization of alloyed $CdTe_xS_{1-x}$ QDSSC

The *J–V* characteristics curves of the assembled $CdTe_xS_{1-x}$ QDSSCs are shown in Fig. 6 for 24 h dipping time and under solar illumination of 100 mW/cm^2. Table 1. summarizes the characteristic parameters for the different x values of alloyed $CdTe_xS_{1-x}$ QDSSCs.

It is clearly seen that as the x value increases, reaching 0.6 for sample (d), the values of J_{sc} and η increase, peaking at 1.54 mA/cm^2 and 0.31%, respectively. These values decrease for sample (e) (1.16 mA/cm^2 and 0.26%) and (f) (1.10 mA/cm^2 and 0.19%). Our earlier measurements of J_{sc} and η for CdTe QDSSCs [2] and CdS QDSSCs [11] having approximately the same size are 1.10 mA/cm^2 and 0.19% and 0.67 mA/cm^2 and 0.18%, respectively. Therefore, Compared to pure CdTe QDs and CdS QDs, $CdTe_xS_{1-x}$ QDs show better photovoltaic performance. Similar results were obtained by Xu. et al. [29]. In their work, they used alloyed $CdSe_xTe_{1-x}$ QDs to sensitize TiO_2 nano-tubes electrode. They tuned the photo electrochemical response and photo conversion efficiency via molar ratio control of $CdSe_xTe_{1-x}$ QDs, and reported that the maximum values of J_{sc} (1.488 mA/cm^2) and η 0.584%) was for 0.6/0.4 of Te/Se ratio, in close agreement with our results of $CdTe_xS_{1-x}$ of Te/S=0.6/0.4. These non-liner changes of J_{sc} and η may result from improved photo-absorption efficiency, and charges separation of $CdTe_xS_{1-x}$ QDs. When Te/S approaches to 0.5/0.5, more interfaces between CdTe and CdS were formed, improving charges separation. Thus, more electrons can be injected to TiO_2 electrode, leading to up-rise of TiO_2 quasi-Fermi level and further increasing J_{sc} and V_{oc} values.

Table 1
J–V characteristics parameters for alloyed $CdTe_xS_{1-x}$ QDSSC (a–f) with different x values.

Electrode	V_{oc} (V) $\pm$0.02	J_{sc} (mA/cm^2) $\pm$0.01	*FF*	Efficiency (η) ($\pm$0.01) %
a	0.49	0.67	0.51	0.18
b	0.45	1.09	0.43	0.21
c	0.45	1.30	0.49	0.29
d	0.47	1.54	0.43	0.31
e	0.45	1.16	0.50	0.26
f	0.50	1.10	0.35	0.19

The values of the V_{oc} is about 0.46 $\pm$ 0.02 V for all alloyed $CdTe_xS_{1-x}$ QDSSCs. Furthermore, V_{oc} value is only dictated by the conduction band (CB) level of TiO_2 NPs and the valance band (VB) of the electrolyte [30]. While the values of *FF* of the assembled cells comprised of $CdTe_xS_{1-x}$ QDs/TiO_2 photo electrode varies between 0.51 and 0.35, as seen in Table 1.

4. Conclusions

Alloyed $CdTe_xS_{1-x}$ QDs of different molar ratio (x) were synthesized using the organometallic pyrolysis method and applied as sensitizers for QDSSCs by the DA technique onto TiO_2 NPs electrode. The open circuit voltages (V_{oc}) is approximately constant (0.47 V) for different x values of the alloyed $CdTe_xS_{1-x}$ QDs. However, it is only dictated by the CB level of TiO_2 NPs and the VB of the electrolyte.

The maximum values of J_{sc} (1.54 mA/cm^2) and η (0.31%) were obtained for the Te/S is 0.6/0.4 of alloyed $CdTe_xS_{1-x}$ QDSSC. The enhancement of J_{sc} and η may result from improving the photo-absorption efficiency, and charges separation of alloyed $CdTe_xS_{1-x}$ QDs. Moreover, When Te/S approaches to 0.6/0.4, more interfaces between CdTe and CdS were formed, improving charges separation. Thus, more electrons can be injected to TiO_2 NPs electrode.

Acknowledgements

The authors wish to thank Taif University for the grant research no. (1/433/1865). The Quantum Optics group at Taif University is also thanked for their assistance during this work. Prof. H. Talaat acknowledges generous support from the Egyptian STDF (ID 377).

References

[1] Y. Xie, S.H. Yoo, C. Chen, S.O. Cho, Mater. Sci. Eng., B 177 (2012) 106–111.
[2] A. Badawi, N. Al-Hosiny, S. Abdallah, S. Negm, H. Talaat, Sol. Energy 88 (2013) 137–143.
[3] H.J. Snaith, A. Stavrinadis, P. DocampoA.A.R. Watt, Sol. Energy 85 (2011) 1283–1290.
[4] K. Tvrdy, P.V. Kamat, J. Phys. Chem. A 113 (2009) 3765–3772.
[5] T. Abdallah, K. Essawy, A. Khalid, S. Negm, H. Talaat, World Acaemy Sci. Eng. Technol. 61 (2012) 533–535.
[6] Z. El-Qahtani, A. Badawi, K. Easawi, N. Al-Hosiny, S. Abdallah, Mater. Sci. Semicond. Process. 20 (2014) 68–73.
[7] K.G.U. Wijayanthaa, L.M. Petera, L.C. Otley, Sol. Energy Mater. Sol. Cells 83 (2004) 363–369.
[8] A. Badawi, N. Al-Hosiny, S. Abdallah, H. Talaat, Mater. Sci.-Poland 31 (2013) 6–13.
[9] J.H. Bang, P.V. Kamat, ACS Nano 3 (2009) 1467–1476.
[10] N. Guijarro, T. Lana-VillarrealI. Mora-SeróJ. BisquertR. Gómez, J. Phys. Chem. C 113 (2009) 4208–4214.
[11] S. Abdallah, N. Al-Hosiny, A. Badawi, J. Nanomater. 2012 (2012) 6.
[12] X. Wu, Sol. Energy 77 (2004) 803–814.
[13] B.-R. Hyun, Y.-W. Zhong, A.C. Bartnik, L. Sun, H.D. Abrun, F.W. Wise, et al., ACS Nano 2 (2008) 2206–2212.
[14] S. Kitada, E. Kikuchi, A. Ohnob, S. Aramakib, S. Maenosono, Solid State Commun. 149 (2009) 1853–1855.
[15] P. Yu, K. Zhu, A.G. Norman, S. Ferrere, A.J. Frank, A.J. Nozik, J. Phys. Chem. B 110 (2006) 25451–25454.
[16] M.-C. Lin, M.-W. Lee, Electron. Commun 13 (2011) 1376–1378.
[17] A. Tubtimtae, M.-W. Lee, G.-J. Wang, J. Power Sources 196 (2011) 6603–6608.
[18] K. Prabakar, H. Seo, M. Son, H. Kim, Mater. Chem. Phys. 117 (2009) 26–28.
[19] I. Barceló, T. Lana-Villarreal, R. Gómez, J. Photochem. Photobiol., A 220 (2011) 47–53.
[20] Y. Zhang, J. Zhu, X. Yu, J. Wei, L. Hu, S. Dai, Sol. Energy 86 (2012) 964–971.
[21] A. SalantM. ShalomI. HodA. FaustA. ZabanU. Banin, ACS Nano 4 (2010) 5962–5968.
[22] N.J. Smith, K.J. Emmett, S.J. Rosenthal, Appl. Phys. Lett. 93 (2008) 043504.
[23] P.V. Kamat, J. Phys. Chem. C 112 (2008) 18737–18753.
[24] D.R. Pernik, K. Tvrdy, J.G. Radich, P.V. Kamat, J. Phys. Chem. C 115 (2011) 13511–13519.
[25] D.V. Talapin, S. Haubold, A.L. Rogach, A. Kornowski, M. Haase, H. Weller, J. Phys. Chem. B 105 (2001) 2260–2263.
[26] S.-H. Choi, H. Song, I.K. Park, J.-H. Yum, S.-S. Kim, S. Lee, et al., J. Photochem. Photobiol., A 179 (2006) 135–141.
[27] G. Syrrokostas, M. Giannouli, P. Yianoulis, Renewable Energy 34 (2009) 1759–1764.
[28] S.N. Alamri, M.S. Benghanem, A.A. Joraid, Adv. Mater. Res. 378-379 (2012) 601–605. (378-379).
[29] T. Xu, F. Zou, Y. Yu, J. Zhi, Mater. Lett. 96 (2013) 8–11.
[30] A. Kongkanand, K. Tvrdy, K. Takechi, M. Kuno, P.V. Kamat, J. Am. Chem. Soc. 130 (2008) 4007–4015.